Numerical Investigation of the Photogating Effect in $MoTe_2$ Photodetectors

J.M. Gonzalez-Medina[†‡], E.G. Marin[†]*, A. Toral-Lopez[†‡], F. G. Ruiz[†‡], A. Godoy[†‡]

[†]Dpto. Electrónica, Universidad de Granada. Av. Fuentenueva S/N, 18071, Granada, Spain
[‡]Pervasive Electronics Advanced Research Laboratory, CITIC, Universidad de Granada, 18071, Granada, Spain
*Dipartamento di Ingegneria dell'Informazione, Università di Pisa, 56122 Pisa, Italy.
Email: jmgonzalme@ugr.es

Introduction

The necessity of overcoming the limitations (e.g. weight, cost and brittleness) of traditional bulk semiconductors employed to build conventional photodetectors, has fueled the interest of the scientific community towards two-dimensional crystals. Its most representative member, graphene [1], with outstanding electrical and mechanical properties, has however a severely limited photoresponsivity due to 1) the lack of bandgap and 2) a reduced carrier lifetime that hardly reaches a few picoseconds [2]. Greater expectations lay on Transition Metal Dichalcogenides (TMDs) [3], the bandgap of which is sensitive to the number of layers. Moreover, TMDs can be stacked forming vertical or lateral heterojunctions [4] giving rise to structures similar to field-effect transistors (FETs) that behave as photodetectors. In this work we theoretically study the optoelectronic properties of a back-gated phototransistor, with its channel formed by few-layer $MoTe_2$, and we focus on the role played by the charges trapped at the channel-insulator interface through the photogating effect [5,6].

Device description and simulation

The device considered here is inspired by the experimental realization described in [7] and is schematically depicted in Fig. 1. The p-type, 8.4 nm-thick $MoTe_2$ lays on top of a bulk SiO_2 substrate (280 nm thick), back-gated by a p-type doped Si. During the fabrication process, impurities, defects and imperfections can be located at the interface between the SiO_2 substrate and the $MoTe_2$, resulting in the presence of a noticeable density of interface traps that are also included in the numerical model. The few-layer $MoTe_2$ flake is ohmically contacted by two metal electrodes acting as source and drain, respectively.

To analyze this structure we have used the SAMANTA code suite [8], which solves self-consistently the 2D Poisson and Drift-Diffusion equations including the effect of light-induced generation, Shockley-Read-Hall recombination and interface and/or bulk traps. The bandgap of $MoTe_2$ has been set to 0.8 eV, corresponding to its bulk form, with an acceptor doping density of $N_A = 1.5\times10^{18}$ cm^{-3}. Electron and hole mobilities have been fixed to 0.3 cm^2/Vs and 5.9 cm^2/Vs, and effective masses to $0.5m_0$ and $0.6m_0$, respectively [7]. The dielectric constant of $MoTe_2$ is set to $10.4\varepsilon_0$. In order to analyze the impact of the photogating effect in 2D-based photodetectors we have considered the presence of hole deep traps following a Gaussian energetic distribution centered at mid-gap and with standard deviation $\sigma = 0.05$ eV. The value of the maximum trap density N_{max} is varied in order to evaluate its effect. The traps are spatially located at the interface between the insulator substrate and the $MoTe_2$ layer (see Fig. 1).

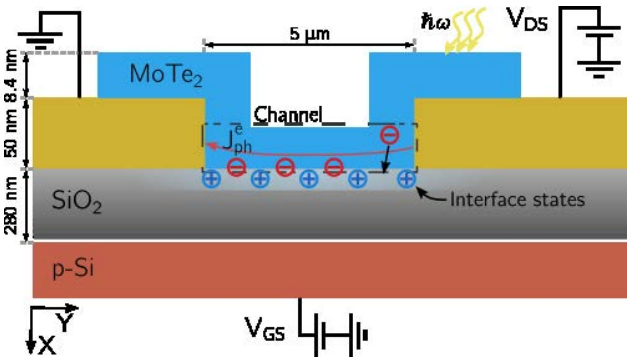

Figure 1 Schematic of the $MoTe_2$ phototransistor with a layer of interface states located between the $MoTe_2$ and the SiO_2.

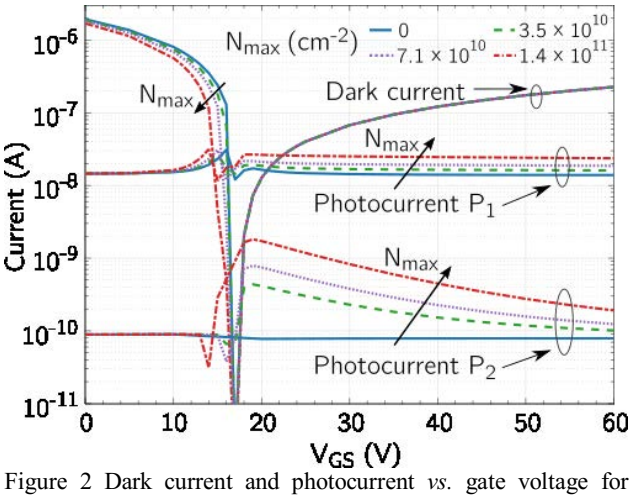

Figure 2 Dark current and photocurrent *vs.* gate voltage for different values of N_{max}, at $V_{DS} = 1$ V, for light power densities: $P_1 = 1$ W/cm^2 and $P_2 = 6$ mW/cm^2.

We have considered two light power densities, $P_1 = 1$ W/cm^2 and $P_2 = 6$ mW/cm^2, so to analyze the traps role and the photogating effect in the 2D-based photodetector under different illumination conditions. The resulting transfer characteristics of the photodetector can be seen in Fig. 2, where the dark current is plotted together with the photocurrents achieved for P_1 and P_2 light power densities, and for different N_{max} values. The influence of the traps is negligible in dark conditions. However, when the device is illuminated, they increase significantly the photocurrent due to the so-called photogating effect [9,10]; in particular, for the lower value of the light power density. In this phenomenon, the trapped holes act as a local gate that augments the channel conductance, resulting into a photoconductive gain. When a high light power density (P_1) is considered, the photocurrent is mainly due to the photoconductive effect, being only slightly enhanced due to the photogating effect. In both high and low light power density cases, the photocurrent remains independent of N_{max} for $V_{GS} < 10$ V, as the hole traps only favor the electron conductivity.

978-1-7281-0940-4/19/$31.00 © 2019 IEEE

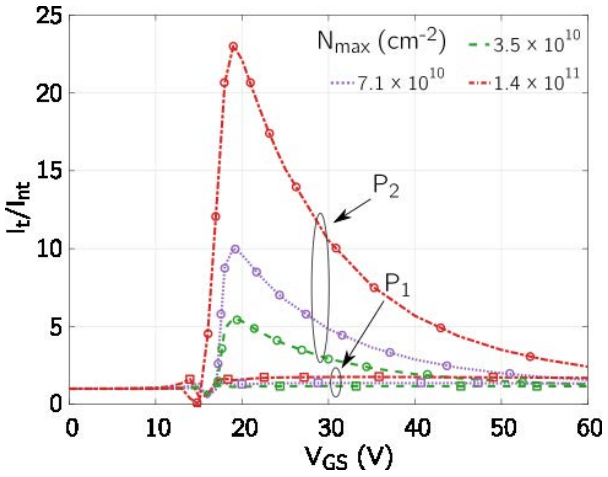

Figure 3 Ratio of the photocurrent calculated for different N_{max} values (I_t) with respect to the case without traps (I_{Int}) for P_1 and P_2 *vs.* V_{GS}.

In the scenario of lower light power density, the contribution of the photoconductive current is smaller due to the reduced amount of photogenerated carriers, and the photogating effect becomes dominant. This contribution is especially remarkable for gate voltages higher than 10 V, where the electron conductivity increases and holes are not strongly repelled from the lower part of the channel by the gate voltage, increasing the probability to be trapped. The relative role of the photogating on the total photocurrent is better appreciated from Fig. 3, that depicts the ratio between the photocurrent when interface traps are considered I_t and when they are not I_{Int}. For the P_2 case, the photocurrent can increase more than one order of magnitude due to the effect of the hole traps. For P_1, on the contrary, the photoconductive contribution is dominant and the effect of the traps is much more smaller. The effect of the charged traps can be better understood in Fig. 4, where the electron and hole photocurrent distributions in the channel are plotted (see inset) for two illumination power densities. The hole current density flows in a similar fashion regardless the light power density. However, the electron photocurrent distribution is different for P_1 and P_2. For P_2 it mainly flows in a sharp region close to the charged interface, due to the photogating effect. On the other hand, for the higher light power density, P_1, the photoconductive effect is dominant due to the large density of photogenerated carriers and the current flow is more homogeneously distributed.

Conclusions

The optoelectronic properties of a $MoTe_2$ phototransistor have been analyzed making use of detailed numerical simulations. The different contributions to the photocurrent has been assessed as a function of the light power density and the hole trap density. In particular, for high light power densities the photoconductive effect dominates the photocurrent, whereas for low power densities the photogating effect has demonstrated its importance, enhancing the overall photocurrent more than one order of magnitude compared with the situation where a perfect interface is assumed.

Acknowledgment

This work has been partially supported by the project TEC2017-89955-P (MINECO/AEI/FEDER, EU) and the grants FPU014/02579 and FPU016/04043. E. G. Marín acknowledges Juan de la Cierva Incorporación IJCI-2017-32297 (MINECO/AEI).

References

[1] A. K. Geim et al. Nature Materials, 6(3):183-191, 2007.
[2] M. M. Furchi et al. Nano Letters, 14, 6165−6170, 2014.
[3] Yi Ding et al. Physica B, 406:2254-2260, 2011.
[4] A. K. Geim et al. Nature, 499:419-425, 2013.
[5] M. Buscema. Chem. Society Rev., 44(11):3691, 2015.
[6] F. H. L. Koppens et al. Nat. Nano., 9(10):780-793, 2014.
[7] H. Huang et al. Nanotechnology, 27, 445201, 2016.
[8] S. Riazimehr et al. ACS Photonics, 6(1):107-115, 2019.
[9] H. Fang et al. Advanced Science, Wiley, 4, 1700323, 2017.
[10] B. Miller et al. Applied Physics Letters, 106, 122103, 2015.

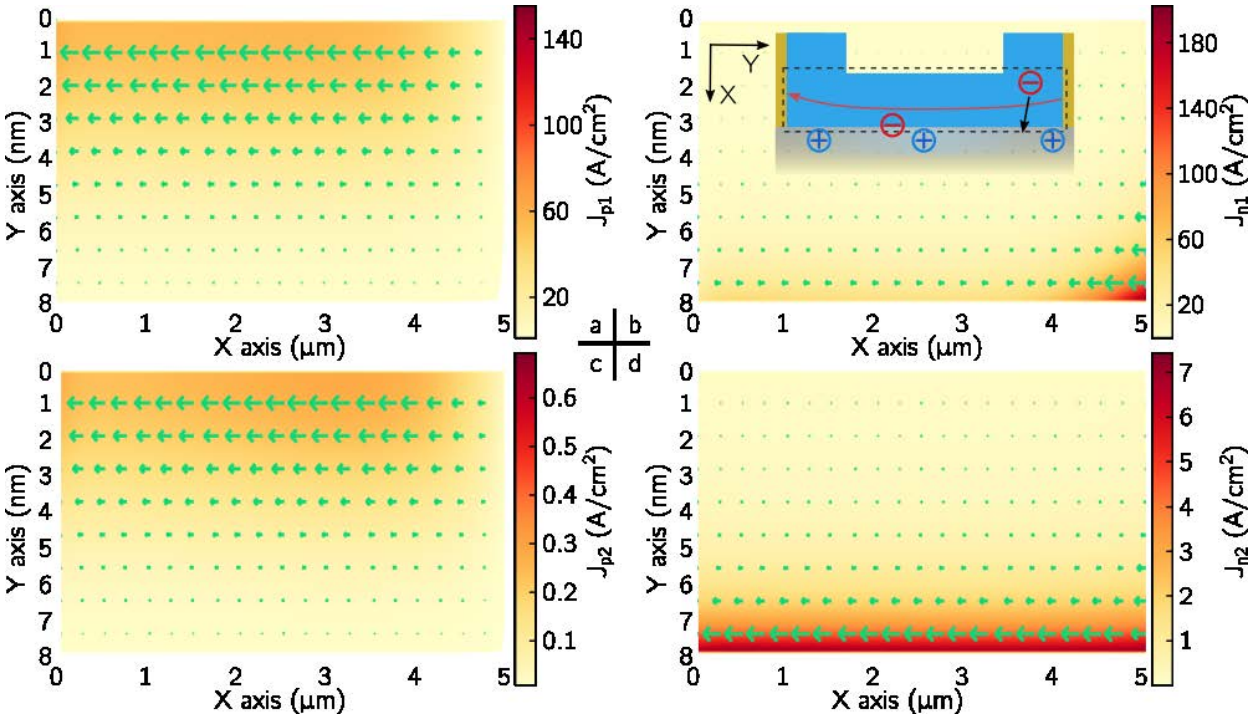

Figure 4 Hole (left column) and electron (right column) photocurrent density distribution in the channel region for P_1 = 1W/cm^2 (top) and P_2 = 6mW/cm^2 (bottom), V_{DS} = 1V and V_{GS} = 19V. Inset: schematic of the device illustrating the zoomed region and the photogating effect .